ISSN 0252-1075
Contribution from IITM
Research Report No. RR-139
ESSO/IITM/SERP/SR/01(2018)/190

A Comparison of Extended-Range Prediction of Monsoon in the IITM-CFSv2 with ECMWF S2S Forecast System

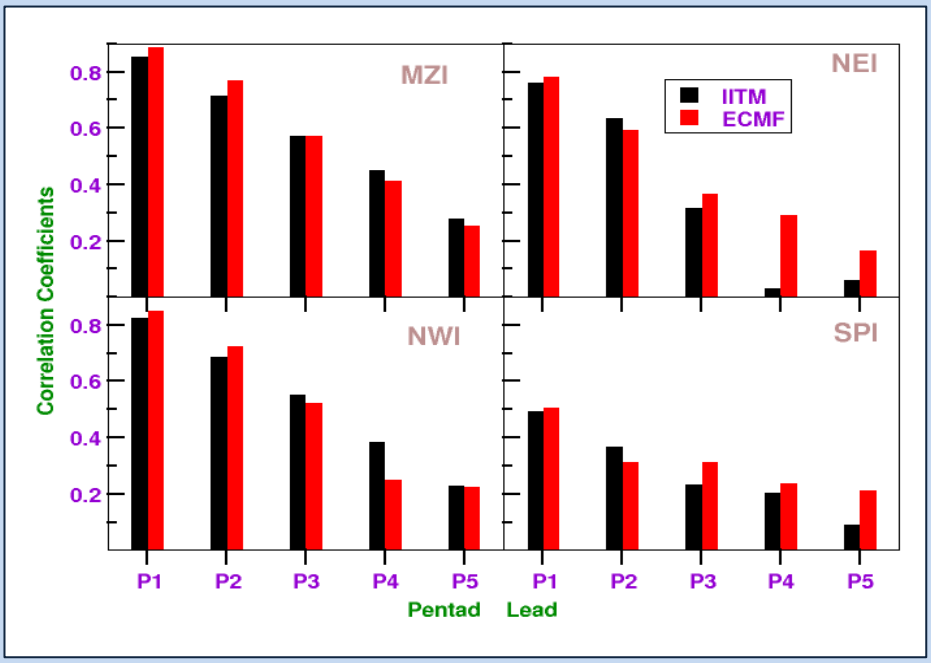

Rajib Chattopadhyay, R. Phani Murali Krishna, Susmitha Joseph, Avijit Dey, Raju Mandal and **A.K. Sahai**

Indian Institute of Tropical Meteorology (IITM)
Earth System Science Organization (ESSO)
Ministry of Earth Sciences (MoES)
PUNE, INDIA
http://www.tropmet.res.in/

ISSN 0252-1075
Contribution from IITM
Research Report No. RR-139
ESSO/IITM/SERP/SR/01(2018)/190

A Comparison of Extended-Range Prediction of Monsoon in the IITM-CFSv2 with ECMWF S2S Forecast System

Rajib Chattopadhyay, R. Phani Murali Krishna, Susmitha Joseph, Avijit Dey, Raju Mandal and **A.K. Sahai**

***Corresponding Author Address:**
Dr. A.K. Sahai
Indian Institute of Tropical Meteorology,
Dr. Homi Bhabha Road, Pashan, Pune – 411 008, INDIA
E-mail: sahai@tropmet.res.in
Phone: +91-20-25904520

Indian Institute of Tropical Meteorology (IITM)
Earth System Science Organization (ESSO)
Ministry of Earth Sciences (MoES)
PUNE, INDIA
http://www.tropmet.res.in/

DOCUMENT CONTROL SHEET

Earth System Science Organization (ESSO)
Ministry of Earth Sciences (MoES)
Indian Institute of Tropical Meteorology (IITM)

ESSO Document Number
ESSO/IITM/SERP/SR/01(2018)/190

Title of the Report
A Comparison of Extended-Range Prediction of Monsoon in the IITM-CFSv2 with ECMWF S2S Forecast System

Authors
Rajib Chattopadhyay, R. Phani Murali Krishna, Susmitha Joseph, Avijit Dey, Raju Mandal, A.K. Sahai

Type of Document
Scientific Report (Research Report)

Number of pages and figures
41, 12

Number of references
54

Keywords
IITM-Extended range prediction system, ECMWF Extended Range Forecast, Skill Comparison, S2S data

Security classification
Open

Distribution
Unrestricted

Date of Publication
January 2018

Abstract
The current study compares the skill of Indian Institute of Tropical Meteorology (IITM) generated real-time forecast with that of the skill of European Centre (ECMF) forecast over different spatial scales and different months during the monsoon season. IITM forecast can give a skill comparable to ECMF forecast as compared to the observation over most of the meteorological subdivision during the monsoon months of June to September. In both the models skill is reduced during the peak monsoon months (July and August). Such reduced skill could be attributed to the high spatial variance of monsoon rainfall during the month of July and August. Thus, the dependence of skill in the climatological mean state of monsoon in two models requires future attention.

Summary

Error growth in climate forecast with the increase in lead-time is an inevitable consequence of nonlinearity and chaos. Study of error growth focusing strictly on the extended range or 10-20 day in advance, a time scale not coming within the purview of weather scale or the seasonal prediction scale is rare. While no rule of thumb to reduce error growth has come up, some headway has been made through a new “bias correction” technique in the NCEP-CFSv2 forecast runs made in Indian Institute of Tropical Meteorology (IITM).

Studying forecast error is critical to understand the model performance. The forecast error is attributed to two important factors: (a) errors in initial conditions and (b) errors in model physics and dynamics. It is easy to get an idea of systematic model error if the forecast of two different modeling systems is compared. The current study focuses on the comparison of forecast skill and error growth of real-time forecasts from IITM-ERPS with a completely different forecast set up: the European center (ECMWF) ERPS.

The study brings a glaring commonality in results from both frameworks when the individual summer monsoon months are forecasted: The skill of both the models at extended range lead-time is significantly dependent on climatological mean state during the monsoon time in the sense that the forecast skill decreases faster during July and August as compared to June and September. Thus, the error growth in monsoon is dominated by the climatological phase of monsoon in two different modeling frameworks, a result that warrants further theoretical clarification in the climate community.

Contents

1. Introduction

The loss in prediction skill of a climate forecast system as the lead-time advances from a starting time is a hurdle that every forecaster face while dealing with real-time forecast since the time of Richardson's effort to forecast mid-latitude weather in the 1940s and 1950s (Charney et al. 1950; Macrae 1999). The cause is well known: from the effect of noise to non-linearity to the chaotic evolution of predictands all could lead to this loss of mathematical foresight to a great extent (Lorenz 1963, 1965; Palmer 1993; Lorenz 1993; Eriksson et al. 2004). Theories to improve the prediction skill in real-time, however, are not many and mainly depends on criteria to improve initial and boundary conditions in the seasonal forecasting models (Reichler and Roads 2003; Palmer and Anderson 1994). For operational seasonal prediction (3-4 monthly averaged forecast), *Charney-Shukla Hypothesis* is a well studied one and is applicable to tropical climate forecast (Charney and Shukla 1981; Shukla 1998). For operational weather prediction (up to five to seven days), improving the initial condition to run a forecast model based on Lorenz's hypothesis is also well explored (Palmer et al. 2005; Palmer 1993; Bauer et al. 2015). In these scales, forecasts of several features are improved a lot as compared to the skill existing at the time when it was first conjectured more than a century ago (Abbe 1901; Bauer et al. 2015). However, once the forecast horizon is expanded beyond weather scale, but is much less than the seasonal scale, skill of forecast gets worse and in spite of existence of theoretical predictability of intraseasonal scale, models do struggle to perform well under various situations (Jung et al. 2010; Baldwin 2003; Palmer 1993; Palmer et al. 1990). For operational purpose prediction beyond weather scale, especially prediction in the extended range time-scale (primarily 15-20 day in advance but could be taken as time-scale less than a

month) requires special mention which by far has given strong hope for predicting intraseasonal oscillations owing to existence of theoretical and operational predictability of Madden-Julian Oscillations or MJOs (Waliser et al. 2003a,b; Vitart 2014; Vitart et al. 2007) and monsoon intraseasonal oscillation or MISOs (Goswami and Xavier 2003; Neena and Goswami 2010; Chattopadhyay et al. 2008).

In the intermediate extended range time-scale, while the role of the initial condition is undisputed (Palmer 1993; Jung et al. 2010), the role of boundary condition e.g. air-sea interaction and sea surface temperature is also recently been shown to be important (Abhilash et al. 2014, 2015). A bias-corrected sea surface temperature (SST) from a coupled general circulation model (CGCM)used as an input to atmospheric component of the same general circulation model (AGCM), for example, can be important in improving the extended range prediction skill when implemented in a multi-model and multi-ensemble (MME) framework (Sahai et al. 2015).

Statistical studies on extended range prediction as well as predictability of atmospheric flow give emphasis on the role of non-linearity and role of stochasticity/chaos as the main sources of the problem(Goswami and Xavier 2003; Webster and Hoyos 2004; Borah et al. 2013). In this context, the role of initial conditions becomes important. Initial conditions could determine the asymmetric or non-identical temporal evolution from one state of initialization to another. For example, low rainfall states (or negative departures from climatology or the *break phases*) could be more predictable than a prediction of higher rainfall states (or the

positive departures from climatology or the *active phases*)(Goswami and Xavier 2003; Taraphdar et al. 2010).

Initial conditions could be considered as the instantaneous weather information from which a forecast model start running. The growth rate of error from an initial condition with the advancement of the lead-time is traditionally assumed to be *exponential* (until they saturate) from any initial state. That is the null hypothesis is, whatever the initial weather state is, error from multiple forecast runs should increase with more or less similar positive "*acceleration*" with lead-time or the errors come from a similar statistical distribution.

Is this conclusion true under all circumstances? There is no clear evidence so far that how statistically certain initial conditions could be more predictable than the other, although experiments with initial conditions say so (Toth and Kalnay 1993; Palmer 2000). Or in other words, certain instantaneous weather states used as input to the model as initial conditions have more memory than the other so that error grows at less positive acceleration rate leading to longer memory process. The assumption is that the techniques should be made available so that the initial conditions generated through data assimilation should nudge more closely to the "real" weather state. The possibility arises that there could be cases when the initialization (assimilation) method is more efficient than some other cases. These *more efficient states* or *long memory initial states* could be due to the role of boundary condition in the form of air-sea interactions in the extended range scale rather than a random initial condition.

Based on the recently developed extended range prediction framework at Indian Institute of Tropical Meteorology (IITM) forecasting of Indian summer monsoon in the extended

range has been recently made operational by Indian Meteorological Department. Operational predictions would be more useful if a systematic statistics of long memory initial states are given. Clear and quantitative demonstrations of these long memory initial states for the Indian summer monsoon season are still missing. If some states (initial conditions) have systematic long memory, those could be giving a systematic improvement in prediction skill. This could be important for monsoon forecasts as it would help the operational forecasters in assigning confidence metric to their forecasts for those initial states which have systematic long memories.

In this study we wish to substantiate this feature of existence of some initial states with systematic long memories in monsoon forecast and try to link it with climatological mean state of monsoon: larger predictability could be achieved in extended range prediction during June and September (traditionally *low (monthly) mean* rainfall but having *strong* amplitude of intraseasonal oscillation (ISO) *variance*) than the July and August (with *high mean* rainfall and *high ISO variance*). This variation of extended range prediction skill is independent of modeling framework as we show this result based on the NCEP-US based CFSv2 derived extended range forecast run at IITM and the ECMWF based extended range forecast. ECMWF forecasts have shown large improvements in operational skill due to a reduction in the initial condition error together with model improvements(Magnusson and Kallen 2013). Hence the similarity in the monthly variation in extended range prediction skill that is independent of modeling framework raises the question on whether the physical processes represented in the model are sufficient to represent seasonal mean monsoon during the peak monsoon season over Indian region. While the answer to this question is not simple, the evidence those are presented here are

overwhelming that the error growth of the monsoon extended range forecast system when it is in seasonally peak phase is not well understood. Additionally, the study induces hope of better quantification of extended range prediction of monsoon on regional scales, which are often important for several operational purposes.

2. Data, Model, and Methods

The World Weather Research Programme/World Climate Research Programme (WWRP/WCRP) has initiated the program on subseasonal to seasonal (S2S) prediction with an objective to understand the subseasonal to seasonal timescale and the forecast skill (Vitart et al. 2016). With an aim to understand and compare the prediction skill of IITM ERPS, we have considered the S2S ECMWF ensemble forecast (CY41R2 version) data (hereafter ECMF ENS) which has 11 ensemble members. In this study, we have considered from May 11th to Sep 28th reforecast for 14 years (2001-2014).

The IITM ERPS use the National Centre for Environmental Prediction, US (NCEP) Climate Forecast System model (CFS) version 2 (Saha et al. 2014), the coupled model and the atmospheric model in CFS namely the Global Forecast System (GFS) forced with the bias-corrected CFS-forecasted SST (hereafter GFSbc) at two resolutions: at T126 (CFS126) and at T382 (CFS382) spectral truncations. The *analyses* for creating the initial conditions for the model are obtained from NCDC server of National Center for Environmental Information (NCEI), USA. It is then perturbed and a pull of initial condition (IC) is created for each of the ensembles. The perturbation method essentially is derived based on adding random numbers to each grid point tendency term for any variable of interest χ: $\chi'(x,y,z,t) = \chi(x,y,z,t) + \alpha \frac{\partial \chi(x,y,z,t)}{\partial t}$. $\boldsymbol{\alpha}$

is a small random number ($-1<\alpha<1$). For more details refer Abhilash et al., (2013) and Abhilash et al., (2015). The IC generation method follows similar logic as defined in (Buizza et al. 1999).

To compare evenly with ECMF ENS, the total number of ensembles members considered for computing the multi-model multi-ensemble (MME) from IITM forecast runs in this study is 11: 3 from each of CFS126, CFS382 and GFSbc126 (one run is using unperturbed original analysis and two using perturbed analysis) and 2 from GFSbc382 (one run is using unperturbed original analysis and one using perturbed analysis).The unperturbed or the control run is made by directly using the real-time analysis IC downloaded from NCEP, defining the CFS based Grand Ensemble Prediction System (CGEPS) runs which also referred as IITM MME hereafter. Abhilash et.al. [2015] has demonstrated that in the IITM MME skill, spread-error relationship and the probabilistic prediction of active (above normal) spells, break (below normal) spells has improved. The reforecast or hindcast is made for the whole monsoon season (June to September) for the years 2001-2014 starting with 16th May for any year and prediction is given for next 45 days. Model run is made after every five-day interval. In this paper apart from IITM MME, individual models (CFS126, CFS382) are also considered to investigate the role of individual NCEP-CFS/GFS model fidelity on the skill. While comparing the individual model to ECMWF forecast runs, the same 11 members of the individual model (CFS126, CFS382) are considered.

The IITM MME forecast runs with a five-day interval from May 16 of every year for 45 days, while the ECMWF runs every Monday/ Thursday of the week of that year on the fly. Following this, the numbers of forecast dates are 31 and 41 for IITM and ECMWF respectively

with the exactly matching dates are 8. For the dates where the ECMF forecast initial date does not match and has a lead of 1 /2/3 days with respect to the IITM MME, then the corresponding forecasted lead days (1/2/3) of IITM MME are matched with the dates of ECMF respectively to be assumed as the forecast start date. The skill plots at a time will be shown by five days (pentad) averaging as has been used in several earlier studies based on this model. Thus forecast at pentad 1 (P1) will be defined as the average of forecasts for the days from 1-5, similarly, for P2, it is forecast average for lead day 6-10 and so on.

The verification of forecast skill is made using India Meteorological Department's (IMD) station data that is gridded and merged with TRMM derived rainfall data. This IMD-TRMM merged rainfall data (Mitra et al. 2009) is used as "observation" data.

3. Results

The skills of the individual component of the models (CFS126 and CFS382) are compared with ECMF ENS in **Fig.1.** The plot shows the skill over 4 homogeneous regions (refer supplementary Figure **S1**), namely *Monsoon Zone of India (MZI), North East India (NEI), Southern Peninsular India (SPI) and Northwest India (NWI).* It may be seen that the skills of extended range forecast in pentad P3, P4 and P5 is much improved in ECMF ENS than the IITM-CFST126 or the IITM-CFST382 for the *MZI, NEI* and the *SPI*. Over *NWI*, it is not significantly different in IITM CFS run and the ECMF ENS run. If CFS126 is compared with CFS382 for these homogeneous regions we can see that the skill up to P3 lead-time is improved in the high resolution (CFS382) run as compared to the low resolution or CFS126 run. For the 4th and 5th pentad forecast, the skill is comparable in CFS126 and CFS382, although the correlation is

markedly low as compared to P1 lead-time. For NWI CFS382 is better up to P4 lead-time. The lack of skill of the individual component model in IITM CFS run is partly overcome when a multi-model and multi-ensemble version of the forecast is created. We plot the same in **Fig.2,** which shows the skill for the result from MME version of the run. The MME is created by taking simple averaging of all the 11 ensemble members. It may be seen that the skill is improved and is comparable to ECMF ENS run up to the fifth pentad over monsoon zone (MZI) and northwest India (NWI). The skill is considerably improved and is comparable to ECMF over north east India (NEI) up to the third pentad in advance. ECMF ENS shows considerable skill in 4th and 5th pentad over NEI. Over the south peninsular part of India (SPI), the ECMF skill is comparatively better in all the 5 pentads shown here. The improvement in skill is coming solely due to the creation of MME and not due to bias-corrected SST-forced run of GFSbc alone. The skills of GFSbc are not always better (especially over the ocean). That the best skill is achievable only through MME and not due to an individual component of the model is already demonstrated in (Abhilash et al. 2014).

The deterministic skill as discussed above may not be very useful when skill score is low. We next show a probabilistic skill score (the briar skill score) which is given in **Fig. 3.** *Brier skill score* is computed by taking an equal number of ensemble members (eleven) for each of the component models (CFS126 and CFS382). Only the MME version (IITM MME) is created by taking lesser number of ensemble members from each model but totaling to eleven to make it comparable with ECMF ENS. So each bar is computed based on equal sample size**.** For the above normal category, the skill at 3rd and 4th pentad are comparable, although ECMF has

better skill in first two pentad lead-time. Similarly, for below normal category, the 3rd and 4th pentad forecast compare well with the ECMF ENS forecast.

In order to gain an insight of the prediction of the large-scale fields, monsoon intraseasonal oscillations (MISOs) are considered next. Predictions of MISOs are important component of any extended range forecasting system as its quasi-periodicity provides the forecast skill beyond weather scale which has several practical applications and has been attempted in the past through statistical and dynamical models (Goswami and Xavier 2003; Chattopadhyay et al. 2008; Webster and Hoyos 2004; Sahai et al. 2015, 2013). Like the real-time multivariate ***RMM1*** and ***RMM2*** indices of MJO (Wheeler and Hendon 2004), the prediction of the large scale structure of the MISO is obtained based on the multivariate ***MISO1*** and ***MISO2*** indices derived from principal components of the extended empirical orthogonal function approach (Suhas et al. 2012). We plot the *bivariate correlation* and *bivariate RMSE* of MISO1 and MISO2 indices in **Fig.4** using the similar approach as defined for RMM1 and RMM2 to indicate the skill of MJO (Lin et al. 2008)**.** The bivariate correlation plot (**Fig.4a**) shows that, although the IITM MME improved the lead time of prediction by 4 days (14 days to 18 days when skill falls below significance line) as compared to the individual component models, it is still less skillful than the ECMF ENS. The same is true for the evolution of bivariate root mean square error (RMSE), which is shown as solid curves in **Fig.4b.** The RMSE of IITM and ECMF run diverges faster after 5-6 days with IITM MME shows larger growth of RMSE on a particular forecast day as compared to the ECMF ENS forecast. The inter-ensemble spread for the IITM and ECMF forecast systems, however, grows at the same rate until 16-17 days. After that, however, the spread of IITM forecast system increases while the ECMF ENS forecast system grows at a slower rate as

compared to IITM forecast system. Since the spread of IITM MME grows faster, the ratio RMSE/spread of both the forecast gets comparable to each other. Since the ratio is an indicator of the signal to noise ratio, it shows that at large lead time, the skills tend to become comparable to each other.

3.1 Monthwise Forecast Skill

The month wise forecast skill for the IITM MME and the ECMF ENS are shown in **Fig.5.** It is clear from the plot that at all lead time and for both the IITM and ECMF ENS shows a reduction in prediction skill for the month of July and August as compared to the month of June and September. The reduction in forecast skill indicates that during the peak monsoon months of July and August, when the convective activities are statistically higher in occurrences with very large scale convection and convective cloudiness prevails over the subcontinent, the models fail to capture the same feature. Since, this is true for both ECMF ENS and IITM MME, which have very different physics and parameterization, it is speculated that forecast runs from both the versions may have the systematic errors of similar nature. During monsoon multi-scale organization of convection is a common feature and occasionally it is seen that the synoptic events are clustered within the monsoon intraseasonal oscillations (Goswami et al. 2003). Rain bearing systems in different scales organize in different space and time scales. Such multi-scale organization is more evident in tropical intraseasonal oscillations and forcing of the seasonal cycle to intraseasonal oscillations in tropics is hypothesized (Moncrieff et al. 2012). Since the seasonal forcing is strong during July and August and statistically monsoon intraseasonal oscillations and synoptic scales are also strong during monsoon season (~50 percent of

seasonal mean , (Goswami and Mohan 2001; Goswami et al. 2003; Qi et al. 2008)), these scales can interact strongly and small scale system can grow more efficiently than June and September. Since small-scale systems are inherently having less prediction horizon, the July and August are less predictable than June and September. This reduction in skill is formally discussed in Sec.4.

3.2 Comparison of monthly Forecasts over IMD subdivisions

P1, P2, P3 and P4 forecasts for various subdivisions during JJAS (June to September average) are shown in **Fig.6. Fig.7-10** shows the same plot but for the month of June, July August and September. For the JJAS season as a whole (**Fig.6**), the IITM MME forecast skill pattern looks similar to ECMF ENS. ECMF ENS forecasts, however, shows better skills in the subdivisions of Northeast India during P4 lead-time forecast. The monthly stratified skill plots in **Fig.7-10** shows that for the month of June and September IITM MME system shows better skill over few more subdivisions as compared to ECMF ENS during P3-P4 lead-time. Also, during July and August, the skill is same for both the models. Another thing is notable that except for the month of June, the larger lead-time (e.g. P4) has no predictability in the east-coastal region and the adjoining subdivisions. Such east-west asymmetry in predictability in both the modeling framework is intriguing. East coast receives most rainfall through Bay-of-Bengal systems which are typically cyclonic storms and low-pressure systems such as depressions which are inherently less predictable in longer lead-time. So if the deterministic predictability over these subdivisions is less, it is clear that probabilistic approach would be the most suitable approach for these regions in the extended range.

3.3 Signal to Noise ratio and Predictability of MMEs in monthly as well as seasonal scale

The month wise and subdivision wise plot for the day when the signal falls below noise level is shown in **Fig. 11.** The top panels are for ECMF runs and the bottom panels are for IITM runs. The red colors denote the predictability below 8 days or in the weather range. The Blue shades show the predictability above 12 days and the white shades show the predictability intermediate between these ranges. It is clear that the noise crosses signal much earlier in ECMF runs than IITM runs in most of the subdivisions during June to September. It is clear that for the runs initialized June and September more subdivisions are predictable in the longer range than the July and August runs. Of all the subdivisions the signal remains stronger over North West India and South peninsular India for longer lead-time.

4. Probable Reasons related to loss in operational predictability

The results as shown above, clearly indicates that for intraseasonal extended range forecast, there is similar monthly variation in forecast skill in two different modeling frameworks. The growth of errors from June and September are much slower and noise crosses signal at longer lead times than July and August. This could be related to the fact that there is increased frequency of "wet spells" during July and August reducing the spatial coherence of rainfall pattern during these months (Moron et al. 2017). These probable reasons are discussed below:

4.1 Predictability variability due to inherent Monsoon Annual Cycle

July and August are vigorous monsoon months with several small scales systems (monsoon depressions, lows, and cyclones) form regularly during these two months over the Bay of Bengal. Recently, several studies provide different aspects of evidence regarding predictability during monsoon season. It was shown that the potential predictability limit is large (20-30 days) over Indian region (Neena and Goswami 2010) considering the JJAS season as a whole. However a study by Moron et al., (2017) based on observation indicates "*spatial coherence and correlations between local rainfall and the regional scale monsoon circulation decrease during the core phase of the monsoon between early July and late August.*.". Such changes in spatial coherence, its link with large-scale circulation and its months variations for subregions of India as shown in this study indicates that the spatial scale of formation and interaction of monsoon system with the subgrid or local scale varies from month to month thereby could a cause of reduction in the actual predictability of the system.

4.2 Predictability variability due to internal dynamics of MISO

Since the predictability in the extended range primarily arises due to intraseasonal oscillations, characteristics of monsoon intraseasonal oscillations during July and August could be important for predictions. A recent study (Li et al. 2016) shows that as the seasonal mean progresses, the strength, propagation characteristics and intensity of the monsoon intraseasonal oscillations over the Arabian sea also changes (stronger in June and September and weaker in July and August) which could affect the predictability in July and August when more dominant tropical disturbances (monsoon lows and depressions) with lower predictability dominate. It is,

therefore, necessary to have proper representation of the regional features of monsoon intraseasonal oscillations in operational models during all the monsoon months. In the light of this, it may be seen that the operational predictability limit can be improved for most of the subdivisions over Indian region if the monthly variation in intraseasonal oscillations is captured correctly.

4.3 Predictability variability due to scale interaction and large-scale teleconnection

The reduction of skill during July and August is evident in both the IITM MME and ECMF ENS models which are run with different frameworks and assumptions. Since synoptic scales could be the roadblock to the prediction of large-scale northward propagating intraseasonal oscillations and there are evidence of scale interactions (De 2010) in monsoon, with the preferential growth of synoptic lows and depressions are favored during July and August, it is possible that such scale interaction could be a possible roadblock for sub seasonal extended range forecast that is yet to be accounted for (Taraphdar et al. 2016). In the month wise context, enhance skill in September (or end of the monsoon season) is worth noting. The reason of extended predictability in September could be related to simultaneous ENSO-monsoon relationship during which the association started getting particularly stronger on or after September (Prasad and Singh 1996; Kirtman and Shukla 2000) and Indian Ocean Dipole and the equatorial Indian Ocean wind mode (IOD/EQUINOO) forcing which also mainly strong in September or the end of the season (Pokhrel et al. 2012; Ashok et al. 2004; Nanjundiah et al. 2013).

5. Discussion

This study has compared the prediction skill of both IITM MME and ECMF ENS runs from the perspective of both global (large scale intraseasonal oscillations) and regional forecasting. The bivariate correlations and root mean square errors are computed for the large scale MISO and the correlations for the larger monsoon zones are also shown for the regions where MISO is more active. Similarly, we have computed the subdivision wise correlation skill to get an idea of the regional implications of the extended range forecast. As of the latest version in IITM MME forecast runs, it is clear that the operational predictability is enhanced beyond ten days for many subdivision for all the monsoon months for northwest India and several subdivisions of west-central India and parts of peninsular India.

The improvement in predictability beyond the medium range at the sub-divisional level is an important operational milestone for the forecast of Indian summer monsoon. The extended range prediction system of IITM MME is addressing two challenging issues at the same time. First, it is taking care of uncertainty in the initial condition through a multi-model and multi-ensemble strategy based on the same model. Secondly, the biases in air-sea interaction flux are corrected significantly through the bias corrected GFS runs. This second result is important in the sense that in the coupled model assumptions, there is no direct control over the errors, whereas in the bias controlled GFS runs the climatological GFS bias is decreased when forced with bias corrected sea surface temperature. The paper thus clearly indicates that for operational prediction in the extended range such errors in large-scale fields more effectively “colludes” the extended range forecast. Hence bias correction of large-scale

boundary conditions has to be an integral part of extended range forecast system. Nevertheless, since monsoon rainfall impacts food grain production over Indian region throughout the year (Selvaraju 2003; Abrol and Gadgil 1999) and if June forecast is important for summer (*Kharif)* crops(rice), the September rainfall is important for winter(*rabi)* crops (e.g. wheat and chickpea), the extended range operational skill during June and September could also be effectively used for crop (agriculture) outlook.

Finally, a natural question arises if it is possible to increase the skill more by making a grand average taking both IITM MME and ECMF ENS forecast. The grand ensemble average (i.e. average of IITM MME forecast runs and ECMF ENS forecast runs) skill and the skill of IITM MME and ECMF ENS are plotted in **Fig.12** (top panel) for the MZI region**.** It may be seen that the increase in skill due to grand ensemble average is seen beyond the P2 lead time which adds operational value to the forecast. The *root means square skill score (rmss*) is also shown along the opposite ordinate (line plots), which also shows improvement in skill in higher lead-time as compared to the individual components. The *Brier skill score (BSS)* is also plotted in the bottom panel of **Fig.12.** The plot also shows improvement in the 3rd and 4th pentad as shown in the deterministic plot in the top panel. Nevertheless, such grand ensemble averaged operational forecasts initialized from synchronized ICs would help to bring out the maximum derivable real-time skill from the model.

6. Conclusions

The current study compares the skill of IITM generated real-time forecast with that of the skill of ECMF forecast over different spatial scales and different months during the monsoon season. The most important conclusion from this comparison is that the IITM forecast, when combined as a MME forecast, can give a skill comparable to ECMF forecast as compared to the observation over most of the meteorological subdivision during the monsoon months of June to September. The other important conclusion is that the skill in both the models is reduced during the peak monsoon months (July and August). Both the models are run with the independent framework and have independent parameterization schemes; in spite of this, they show similar variation in skill when monthly variation in skill is considered. Such reduced skill could be attributed to the high spatial variance of monsoon rainfall during the month of July and August. Thus, the dependence of skill in the climatological mean state of monsoon in two models requires future attention.

Acknowledgments The authors wish to thankfully acknowledge Dr. Andrew Robertson, IRI (Columbia, US) and Dr. Frederic Vitart, ECMWF for their helpful comments and suggestion in writing the manuscript. IITM is fully supported by the Ministry of Earth Sciences Govt. India, New Delhi. We thank NCEP, US for analysis datasets and technical support on CFS model. This work is based on S2S data. S2S is a joint initiative of the World Weather Research Programme (WWRP) and the World Climate Research Programme (WCRP). The original S2S database is hosted at ECMWF as an extension of the TIGGE database. We also thank IMD for TRMM and Rain-gauge-merged daily rainfall data.

References

Abbe, C., 1901: The physical basis of long-range weather forecasts. *Mon. Weather Rev.*, **29**, 551–561, doi:10.1175/1520-0493(1901)29[551c:TPBOLW]2.0.CO;2.

Abhilash, S., A. K. Sahai, S. Pattnaik, and S. De, 2013: Predictability during active break phases of Indian summer monsoon in an ensemble prediction system using climate forecast system. *J. Atmospheric Sol.-Terr. Phys.*, **100–101**, 13–23, doi:10.1016/j.jastp.2013.03.017.

Abhilash, S., A. K. Sahai, N. Borah, R. Chattopadhyay, S. Joseph, S. Sharmila, S. De, and B. N. Goswami, 2014: Does bias correction in the forecasted SST improve the extended range prediction skill of active-break spells of Indian summer monsoon rainfall? *Atmospheric Sci. Lett.*, **15**, 114–119, doi:10.1002/asl2.477.

Abhilash, S., and Coauthors, 2015: Improved Spread-Error Relationship and Probabilistic Prediction from CFS based Grand Ensemble Prediction System. *J Appl Meteor Clim.*, 1569–1578.

Abrol, Y. P., and S. Gadgil, 1999: *Rice, in a variable climate*. APC Publications, 260 pp.

Ashok, K., Z. Guan, N. H. Saji, and T. Yamagata, 2004: Individual and Combined Influences of ENSO and the Indian Ocean Dipole on the Indian Summer Monsoon. *J. Clim.*, **17**, 3141–3155, doi:10.1175/1520-0442(2004)017<3141:IACIOE>2.0.CO;2.

Baldwin, M. P., 2003: Stratospheric Memory and Skill of Extended-Range Weather Forecasts. *Science*, **301**, 636–640, doi:10.1126/science.1087143.

Bauer, P., A. Thorpe, and G. Brunet, 2015: The quiet revolution of numerical weather prediction. *Nature*, **525**, 47–55, doi:10.1038/nature14956.

Borah, N., A. K. Sahai, R. Chattopadhyay, S. Joseph, S. Abhilash, and B. N. Goswami, 2013: A self-organizing map–based ensemble forecast system for extended range prediction of active/break cycles of Indian summer monsoon. *J. Geophys. Res. Atmospheres*, **118**, 9022–9034, doi:10.1002/jgrd.50688.

Buizza, R., M. Milleer, and T. N. Palmer, 1999: Stochastic representation of model uncertainties in the ECMWF ensemble prediction system. *Q. J. R. Meteorol. Soc.*, **125**, 2887–2908, doi:10.1002/qj.49712556006.

Charney, J. G., and J. Shukla, 1981: Predictability of monsoons. *Monsoon Dynamics,* Cambridge University Press, 99–109.

Charney, J. G., R. Fjörtoft, and J. Von NEUMANN, 1950: Numerical Integration of the Barotropic Vorticity Equation. *Tellus*, **2**, 237–254, doi:10.1111/j.2153-3490.1950.tb00336.x.

Chattopadhyay, R., A. K, and B. . Goswami, 2008: Objective Identification of Nonlinear Convectively Coupled Phases of Monsoon Intraseasonal Oscillation: Implications for Prediction. *J Atmos Sci*, **65**, 1549–1569.

De, S., 2010: Role of nonlinear scale interactions in limiting dynamical prediction of lower tropospheric boreal summer intraseasonal oscillations. *J. Geophys. Res. Atmospheres*, **115**, D21127, doi:10.1029/2010JD013955.

Eriksson, K., C. Johnson, and D. Estep, 2004: Lorenz and the Essence of Chaos. *Applied Mathematics: Body and Soul: Calculus in Several Dimensions*, K. Eriksson, C. Johnson, and D. Estep, Eds., Springer Berlin Heidelberg, Berlin, Heidelberg, 849–858 http://dx.doi.org/10.1007/978-3-662-05800-8_5.

Goswami, B. N., and R. S. A. Mohan, 2001: Intraseasonal Oscillations and Interannual Variability of the Indian Summer Monsoon. *J. Clim.*, **14**, 1180–1198, doi:10.1175/1520-0442(2001)014<1180:IOAIVO>2.0.CO;2.

——, and P. K. Xavier, 2003: Potential predictability and extended range prediction of Indian summer monsoon breaks. *Geophys. Res. Lett.*, **30**, 1966, doi:10.1029/2003GL017810.

——, R. S. Ajayamohan, P. K. Xavier, and D. Sengupta, 2003: Clustering of synoptic activity by Indian summer monsoon intraseasonal oscillations. *Geophys. Res. Lett.*, **30**, 1431, doi:10.1029/2002GL016734.

Jung, T., M. J. Miller, and T. N. Palmer, 2010: Diagnosing the Origin of Extended-Range Forecast Errors. *Mon. Weather Rev.*, **138**, 2434–2446, doi:10.1175/2010MWR3255.1.

Kirtman, B. P., and J. Shukla, 2000: Influence of the Indian summer monsoon on ENSO. *Q. J. R. Meteorol. Soc.*, **126**, 213–239, doi:10.1002/qj.49712656211.

Li, Y., W. Han, W. Wang, and M. Ravichandran, 2016: Intraseasonal Variability of SST and Precipitation in the Arabian Sea during the Indian Summer Monsoon: Impact of Ocean Mixed Layer Depth. *J. Clim.*, **29**, 7889–7910, doi:10.1175/JCLI-D-16-0238.1.

Lin, H., G. Brunet, and J. Derome, 2008: Forecast Skill of the Madden–Julian Oscillation in Two Canadian Atmospheric Models. *Mon. Weather Rev.*, **136**, 4130–4149, doi:10.1175/2008MWR2459.1.

Lorenz, E. N., 1963: Deterministic Nonperiodic Flow. *J. Atmospheric Sci.*, **20**, 130–141, doi:10.1175/1520-0469(1963)020<0130:DNF>2.0.CO;2.

——, 1965: A study of the predictability of a 28-variable atmospheric model. *Tellus*, **17**, 321–333, doi:10.1111/j.2153-3490.1965.tb01424.x.

Lorenz, E. N., 1993: *The Essence of Chaos*. University of Washington Press, Seattle, US,.

Macrae, N., 1999: *John von Neumann: The Scientific Genius Who Pioneered the Modern Computer, Game Theory, Nuclear Deterrence, and Much More*. American Math. Soc., US,.

Magnusson, L., and E. Kallen, 2013: Factors Influencing Skill Improvements in the ECMWF Forecasting System. *Mon. Weather Rev.*, **141**, 3142–3153, doi:10.1175/MWR-D-12-00318.1.

Mitra, A. K., A. K. Bohra, M. N. Rajeevan, and T. N. Krishnamurti, 2009: Daily Indian Precipitation Analysis Formed from a Merge of Rain-Gauge Data with the TRMM TMPA Satellite-Derived Rainfall Estimates. *J. Meteorol. Soc. Jpn. Ser II*, **87A**, 265–279.

Moncrieff, M. W., D. E. Waliser, M. J. Miller, M. A. Shapiro, G. R. Asrar, and J. Caughey, 2012: Multiscale Convective Organization and the YOTC Virtual Global Field Campaign. *Bull. Am. Meteorol. Soc.*, **93**, 1171–1187, doi:10.1175/BAMS-D-11-00233.1.

Moron, V., A. W. Robertson, and D. S. Pai, 2017: On the spatial coherence of sub-seasonal to seasonal Indian rainfall anomalies. *Clim. Dyn.*, 1–21, doi:10.1007/s00382-017-3520-5.

Nanjundiah, R., P. A. Francis, M. Ved, and S. Gadgil, 2013: Predicting the extremes of Indian summer monsoon rainfall with coupled ocean– atmosphere models. *Curr Sci*, **104**, 1380.

Neena, J. M., and B. N. Goswami, 2010: Extension of potential predictability of Indian summer monsoon dry and wet spells in recent decades. *Q. J. R. Meteorol. Soc.*, **136**, 583–592, doi:10.1002/qj.595.

Palmer, T., and D. Anderson, 1994: The Prospects for Seasonal Forecasting - a Review Paper. *Q. J. R. Meteorol. Soc.*, **120**, 755–793, doi:10.1002/qj.49712051802.

Palmer, T. N., 1993: Extended-Range Atmospheric Prediction and the Lorenz Model. *Bull. Am. Meteorol. Soc.*, **74**, 49–65, doi:10.1175/1520-0477(1993)074<0049:ERAPAT>2.0.CO;2.

——, 2000: Predicting uncertainty in forecasts of weather and climate. *Rep. Prog. Phys.*, **63**, 71, doi:10.1088/0034-4885/63/2/201.

——, Č. Branković, F. Molteni, and S. Tibaldi, 1990: Extended-range predictions with ecmwf models: Interannual variability in operational model integrations. *Q. J. R. Meteorol. Soc.*, **116**, 799–834, doi:10.1002/qj.49711649403.

——, G. J. Shutts, R. Hagedorn, F. J. Doblas-Reyes, T. Jung, and M. Leutbecher, 2005: Representing Model Uncertainty in Weather and Climate Prediction. *Annu. Rev. Earth Planet. Sci.*, **33**, 163–193, doi:10.1146/annurev.earth.33.092203.122552.

Pokhrel, S., H. S. Chaudhari, S. K. Saha, A. Dhakate, R. K. Yadav, K. Salunke, S. Mahapatra, and S. A. Rao, 2012: ENSO, IOD and Indian Summer Monsoon in NCEP climate forecast system. *Clim. Dyn.*, **39**, 2143–2165, doi:10.1007/s00382-012-1349-5.

Prasad, K. D., and S. V. Singh, 1996: Seasonal Variations of the Relationship Between Some Enso Parameters and Indian Rainfall. *Int. J. Climatol.*, **16**, 923–933, doi:10.1002/(SICI)1097-0088(199608)16:8<923::AID-JOC62>3.0.CO;2-5.

Qi, Y., R. Zhang, T. Li, and M. Wen, 2008: Interactions between the summer mean monsoon and the intraseasonal oscillation in the Indian monsoon region. *Geophys. Res. Lett.*, **35**, L17704, doi:10.1029/2008GL034517.

Reichler, T. J., and J. O. Roads, 2003: The role of boundary and initial conditions for dynamical seasonal predictability. *Nonlin Process. Geophys*, **10**, 211–232, doi:10.5194/npg-10-211-2003.

Saha, S., and Coauthors, 2014: The NCEP Climate Forecast System Version 2. *J. Clim.*, **27**, 2185–2208, doi:10.1175/JCLI-D-12-00823.1.

Sahai, A. K., and Coauthors, 2013: Simulation and Extended range prediction of Monsoon Intraseasonal Oscillations in NCEP CFS/GFS version 2 framework. *Curr Sci*, **104**, 1394–1408.

Sahai, A. K., R. Chattopadhyay, S. Joseph, R. Mandal, A. Dey, S. Abhilash, R. P. M. Krishna, and N. Borah, 2015: Real-time performance of a multi-model ensemble-based extended range forecast system in predicting the 2014 monsoon season based on NCEP-CFSv2. *Curr Sci*, **109**, 1802–1813.

Selvaraju, R., 2003: Impact of El Niño–southern oscillation on Indian foodgrain production. *Int. J. Climatol.*, **23**, 187–206, doi:10.1002/joc.869.

Shukla, J., 1998: Predictability in the Midst of Chaos: A Scientific Basis for Climate Forecasting. *Science*, **282**, 728–731, doi:10.1126/science.282.5389.728.

Suhas, E., J. Neena, and B. Goswami, 2012: An Indian monsoon intraseasonal oscillations (MISO) index for real time monitoring and forecast verification. *Clim. Dyn.*, 1–12, doi:10.1007/s00382-012-1462-5.

Taraphdar, S., P. Mukhopadhyay, and B. N. Goswami, 2010: Predictability of Indian summer monsoon weather during active and break phases using a high resolution regional model. *Geophys. Res. Lett.*, **37**, L21812, doi:10.1029/2010GL044969.

——, ——, L. R. Leung, and K. Landu, 2016: Prediction skill of tropical synoptic scale transients from ECMWF and NCEP Ensemble Prediction Systems. *Math. Clim. Weather Forecast.*, **2**, doi:10.1515/mcwf-2016-0002. https://www.degruyter.com/view/j/mcwf.2016.2.issue-1/mcwf-2016-0002/mcwf-2016-0002.xml (Accessed December 14, 2017).

Toth, Z., and E. Kalnay, 1993: Ensemble Forecasting at NMC: The Generation of Perturbations. *Bull. Am. Meteorol. Soc.*, **74**, 2317–2330, doi:10.1175/1520-0477(1993)074<2317:EFANTG>2.0.CO;2.

Vitart, F., 2014: Evolution of ECMWF sub-seasonal forecast skill scores. *Q. J. R. Meteorol. Soc.*, **140**, 1889–1899, doi:10.1002/qj.2256.

——, S. Woolnough, M. A. Balmaseda, and A. M. Tompkins, 2007: Monthly Forecast of the Madden–Julian Oscillation Using a Coupled GCM. *Mon. Weather Rev.*, **135**, 2700–2715, doi:10.1175/MWR3415.1.

Vitart, F., and Coauthors, 2016: The Subseasonal to Seasonal (S2S) Prediction Project Database. *Bull. Am. Meteorol. Soc.*, **98**, 163–173, doi:10.1175/BAMS-D-16-0017.1.

Waliser, D. E., K. M. Lau, W. Stern, and C. Jones, 2003a: Potential Predictability of the Madden–Julian Oscillation. *Bull. Am. Meteorol. Soc.*, **84**, 33–50, doi:10.1175/BAMS-84-1-33.

——, W. Stern, S. Schubert, and K. M. Lau, 2003b: Dynamic predictability of intraseasonal variability associated with the Asian summer monsoon. *Q. J. R. Meteorol. Soc.*, **129**, 2897–2925, doi:10.1256/qj.02.51.

Webster, P. J., and C. Hoyos, 2004: Prediction of Monsoon Rainfall and River Discharge on 15–30-Day Time Scales. *Bull. Am. Meteorol. Soc.*, **85**, 1745–1765, doi:10.1175/BAMS-85-11-1745.

Wheeler, M. C., and H. H. Hendon, 2004: An All-Season Real-Time Multivariate MJO Index: Development of an Index for Monitoring and Prediction. *Mon Wea Rev*, **132**, 1917–1932.

Figure Captions

Figure 1: Comparison of correlation skills of CFS126 and CFS382 with ECMF forecast runs for the pentad 1 (P1) to pentad 4 (P4) lead time. Skill score is based on 11 members from each of ECMF ENS, CFST382 and CFST126 runs.

Figure 2: Comparison of correlation skills of IITM MME and ECMF ENS for the 4 homogeneous regions of India. Skill score is based on 11 members from each of ECMF ENS and IITM MME.

Figure 3: Brier Skill score for the monsoon zone for the above normal and below normal categories for the IITM MME and the ECMF ENS. Also shown the same for individual component models. Skill score is based on 11 members taken from each of the models.

Figure 4: (a) The bivariate correlation and (b) the root mean square error (RMSE) and spread for the ECMF-MME, IITM-MME and individual component models.(c) The ratio of Bivariate RMSE and spread as a function of lead day.

Figure 5: Monthwise variation in prediction skill for the ECMF and IITM runs.

Figure 6: Figure 6: Subdivision wise skill for the June-September (JJAS) season. Left columns show the skill for ECMF ENS for P1—P4 pentad lead time (top to bottom). Right columns show the skill for IITM MME for P1—P4 pentad lead time (top to bottom).

Figure 7: IMD Subdivision wise skill for the month of June for the IITM and ECMF forecast runs at each of the P1-P4 lead times.

Figure 8: Same as figure 8 but for the month of July.

Figure 9: Same as figure 8 but for the month of August.

Figure 10: Same as figure 8 but for the month of September.

Figure 11: subdivision wise spatial pattern of the days (shaded) in ECMF and IITM runs when the signal is equal to noise.

Figure 12: (top) Deterministic skill scores (cc and rmss) for the all of the IITM and ECMF combined (COMB), IITM MME and ECMF ENS forecasts and, (bottom) Brier skill score for the core monsoon zone of India (MZI).

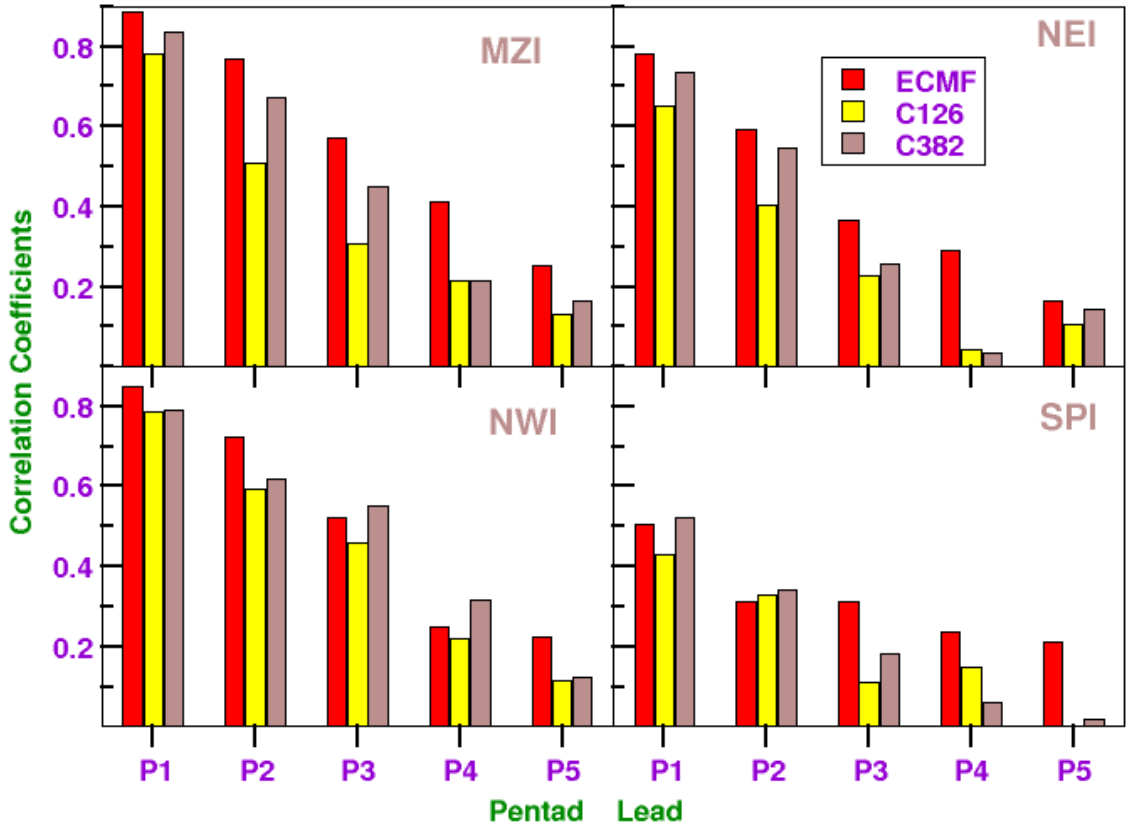

Figure 1: Comparison of correlation skills of CFS126 and CFS382 with ECMF forecast runs for the pentad 1 (P1) to pentad 4 (P4) lead time. Skill is shown for the four homogeneous regions of India. Skill score is based on 11 members from each of ECMF ENS, CFST382 and CFST126 runs.

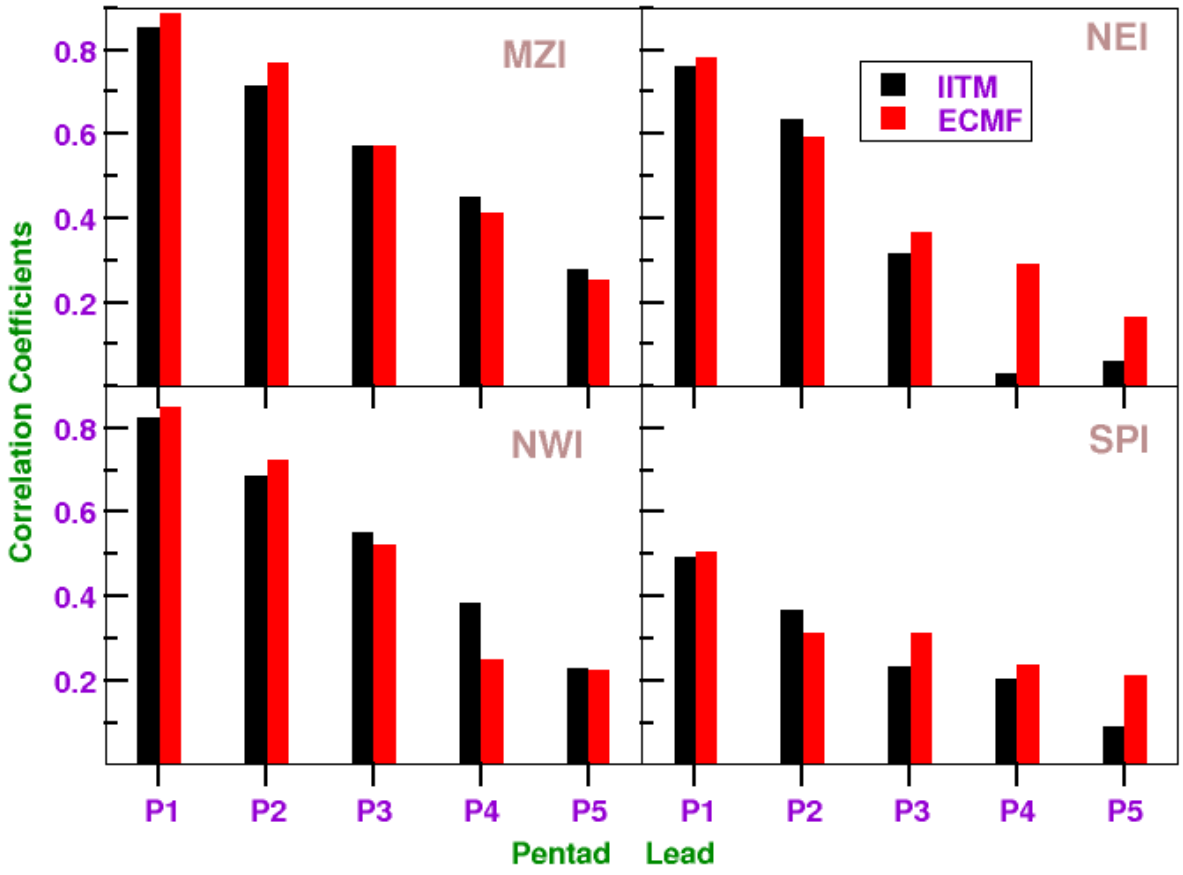

Figure 2: Comparison of correlation skills of IITM MME and ECMF ENS for the 4 homogeneous regions of India. Skill score is based on 11 members from each of ECMF ENS and IITM MME.

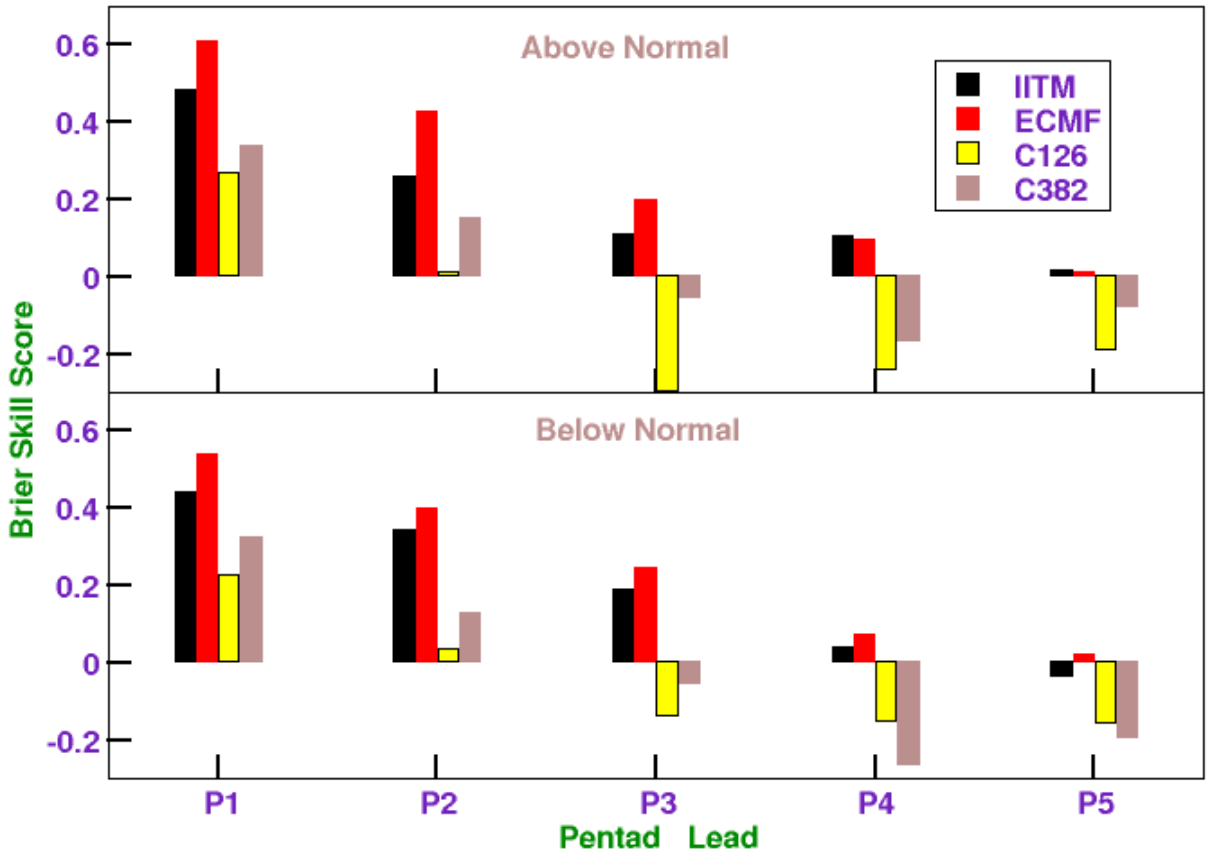

Figure 3: Brier Skill score for the monsoon zone for the above normal and below normal categories for the IITM MME and the ECMF ENS. Also shown the same for individual component models. Skill score is based on 11 members taken from each of the models.

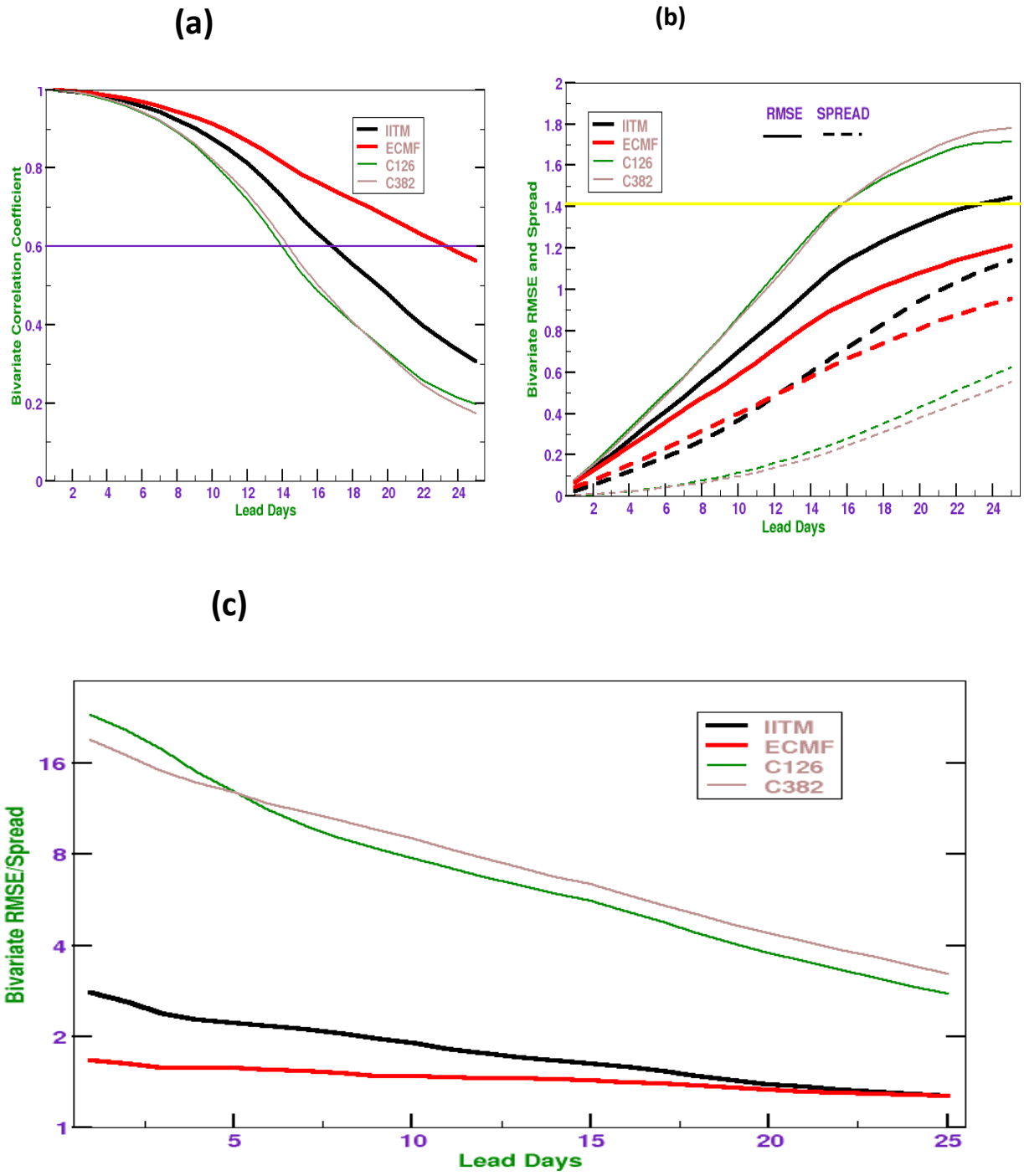

Figure 4: (a) The bivariate correlation and (b) the root mean square error (RMSE) and spread for the ECMF-MME, IITM-MME and individual component models.(c) The ratio of Bivariate RMSE and spread as a function of lead day.

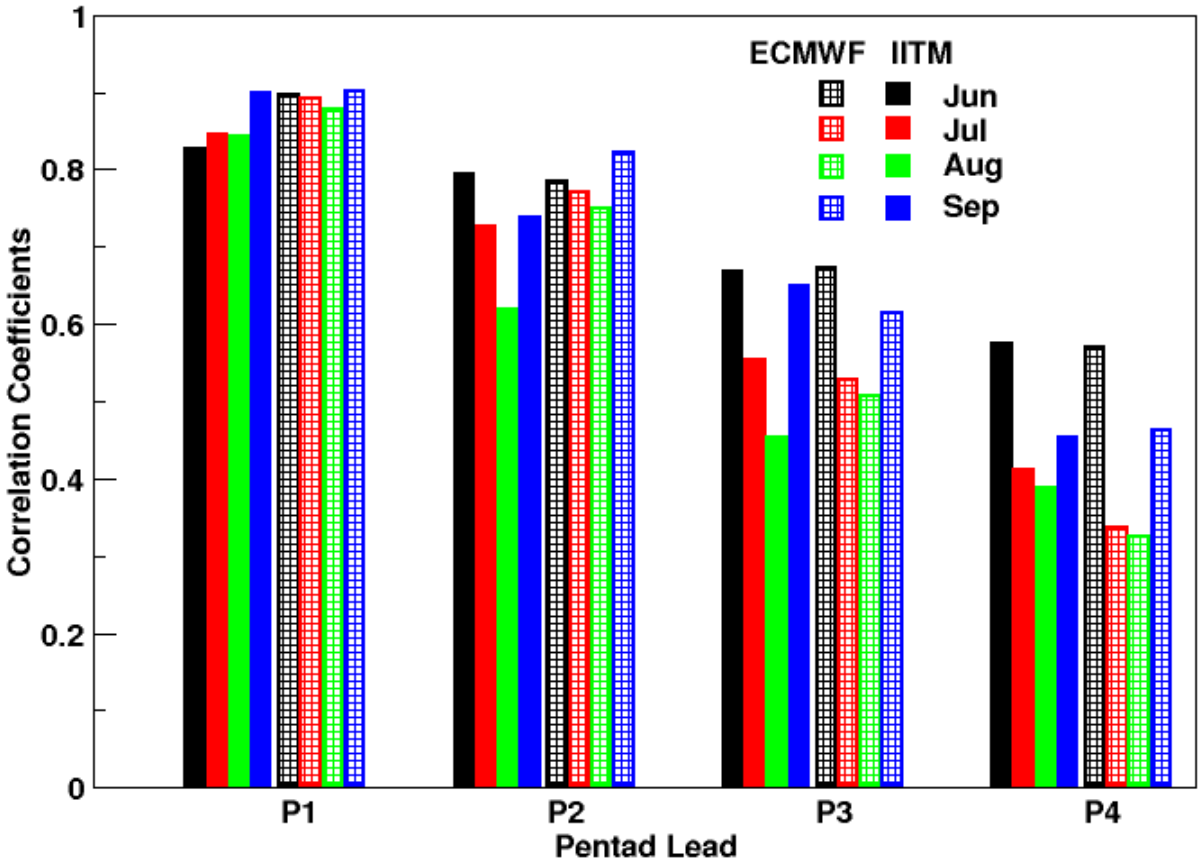

Figure 5: Monthwise variation in prediction skill for the ECMF and IITM runs.

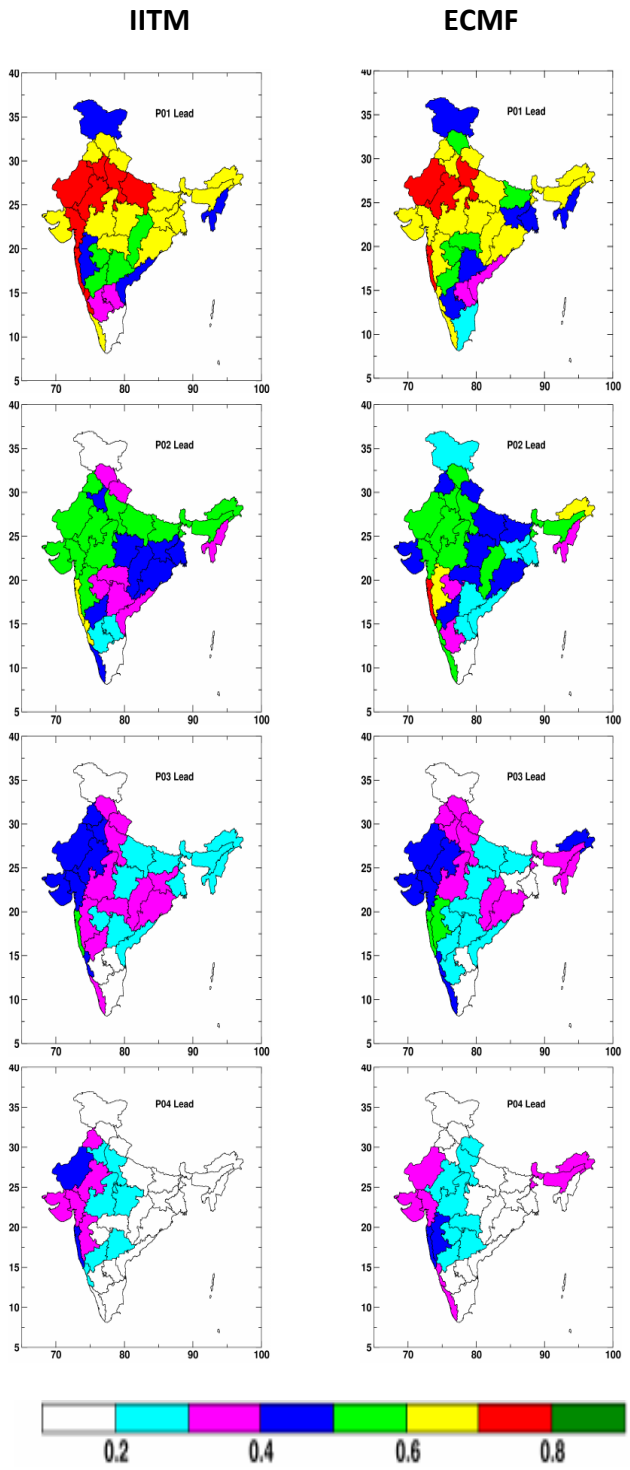

Figure 6: Subdivision wise skill for the June-September (JJAS) season. Left columns show the skill for IITM ENS for P1—P4 pentad lead time (top to bottom). Right columns show the skill for ECMF MME for P1—P4 pentad lead time (top to bottom)

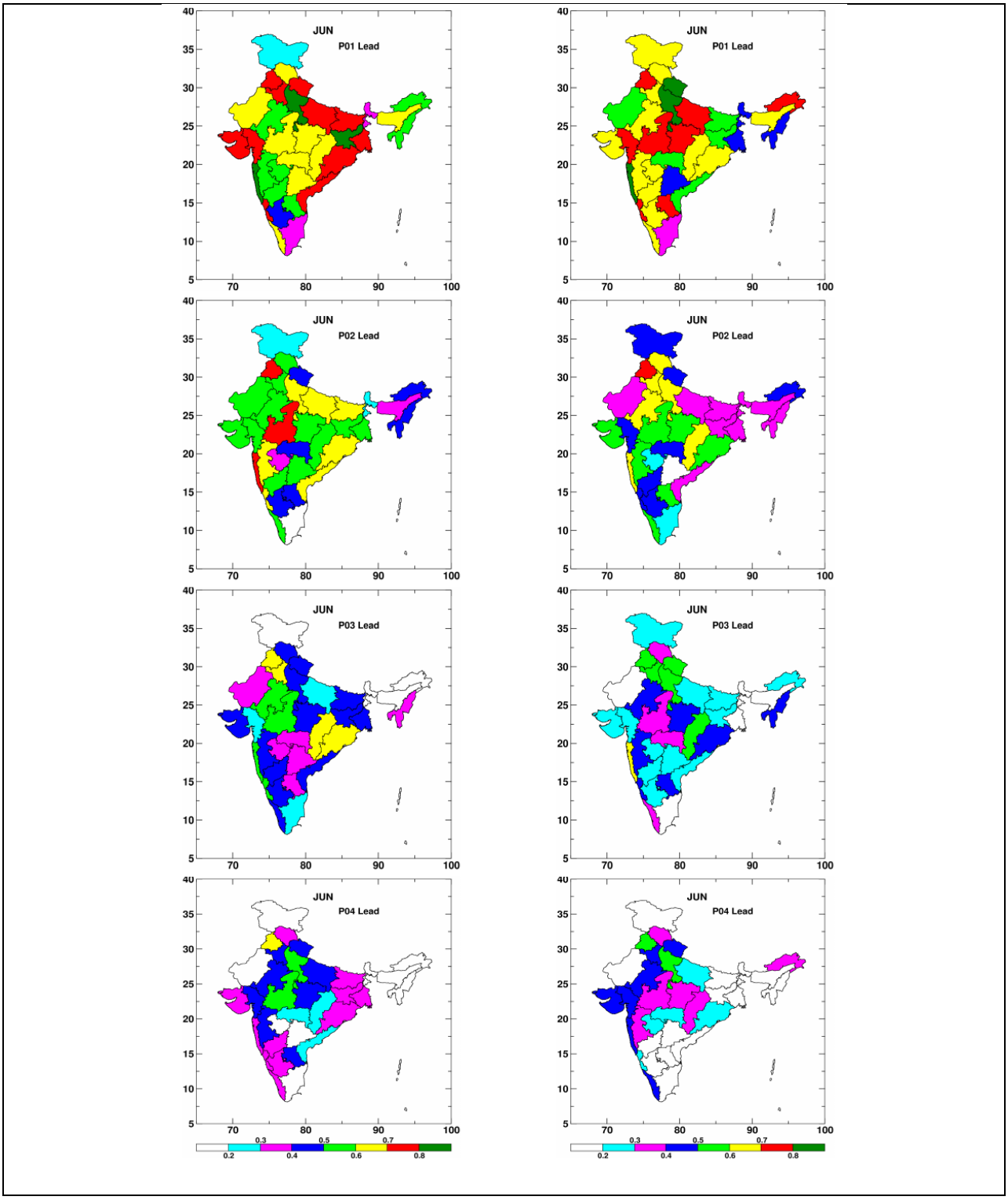

Figure 7: IMD Subdivision wise skill for the month of June for the IITM (left) and ECMF (right) forecast runs at each of the P1-P4 lead times.

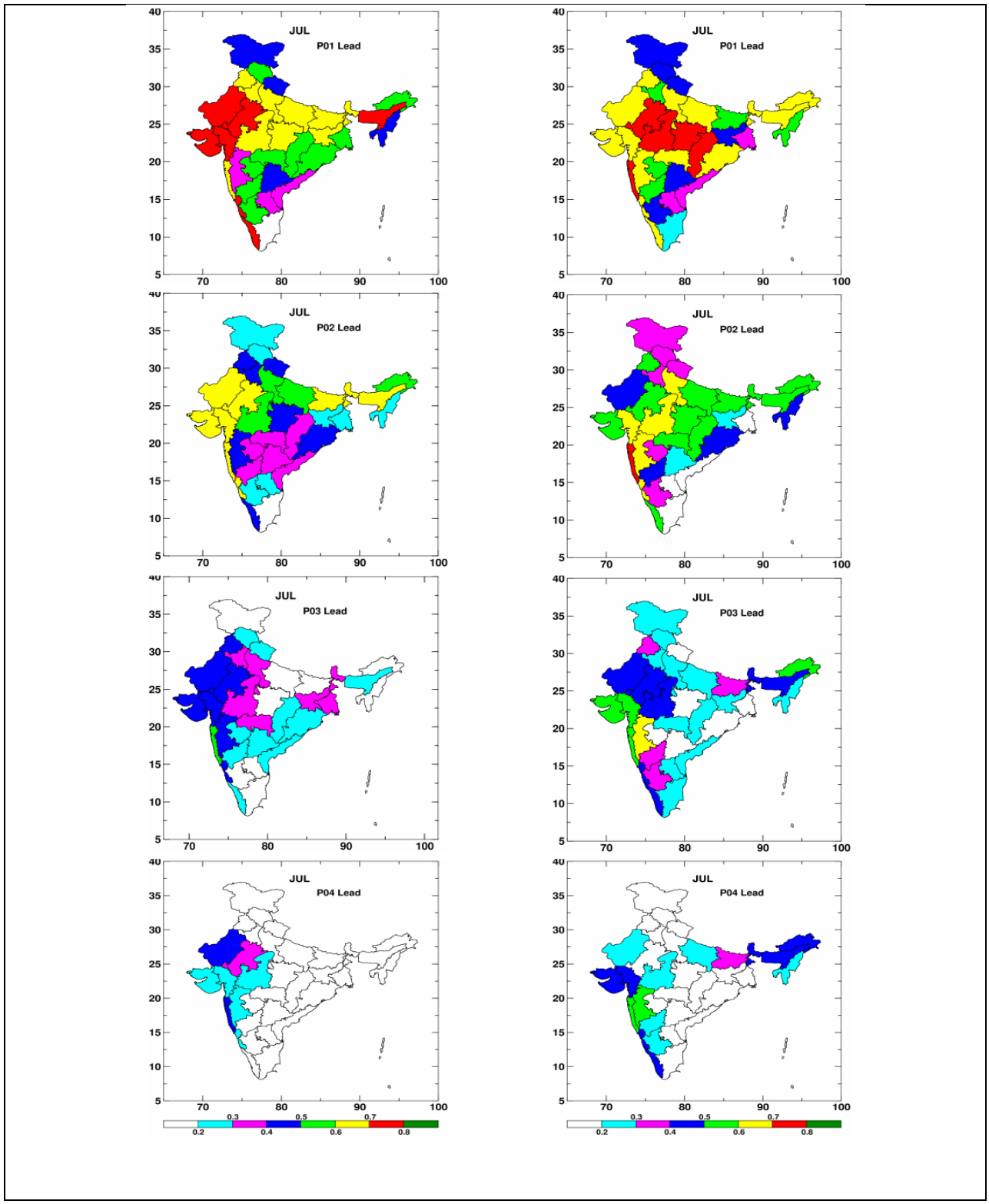

Figure 8: Same as figure 7 but for the month of July.

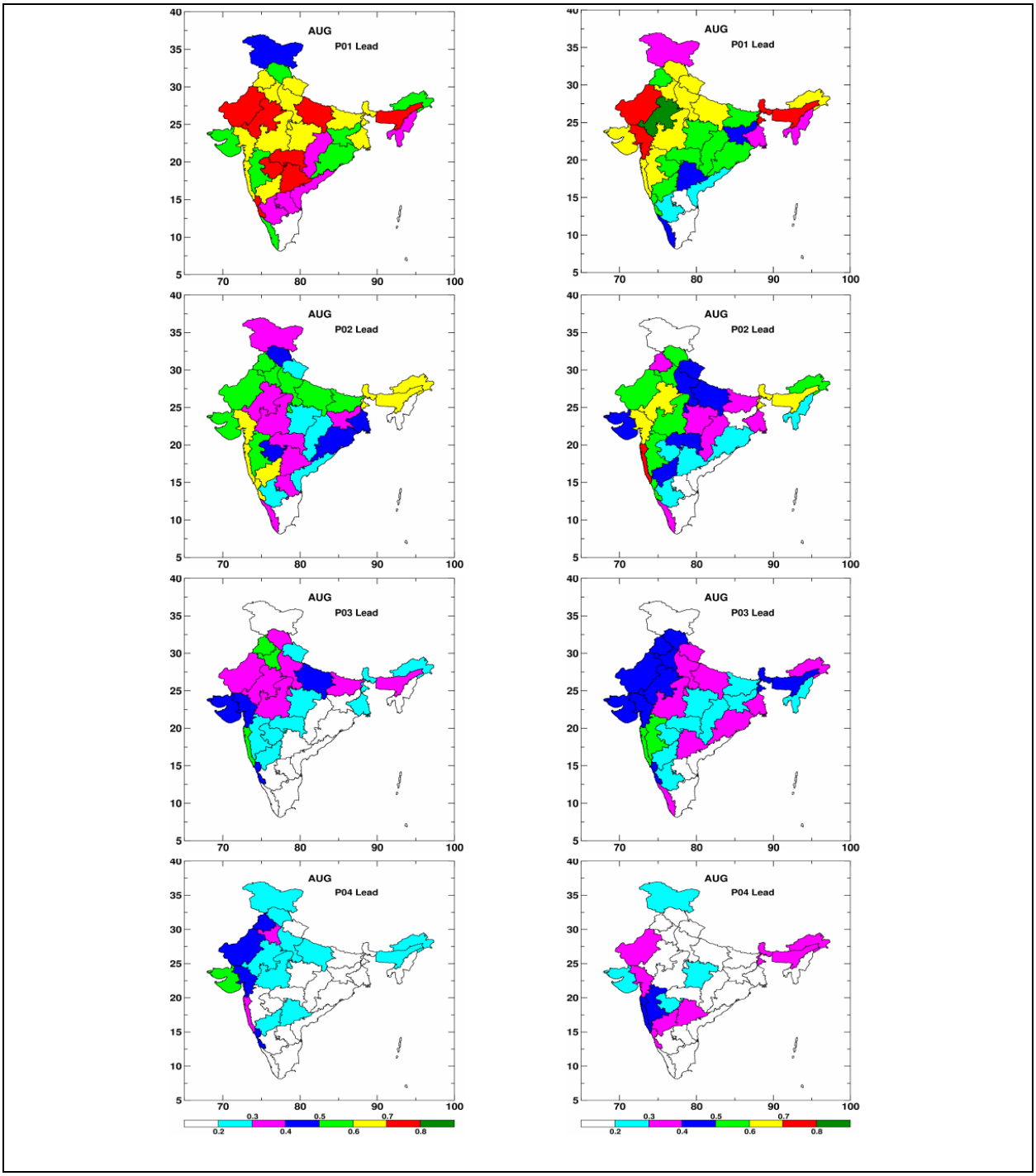

Figure 9: Same as figure 8 but for the month of August.

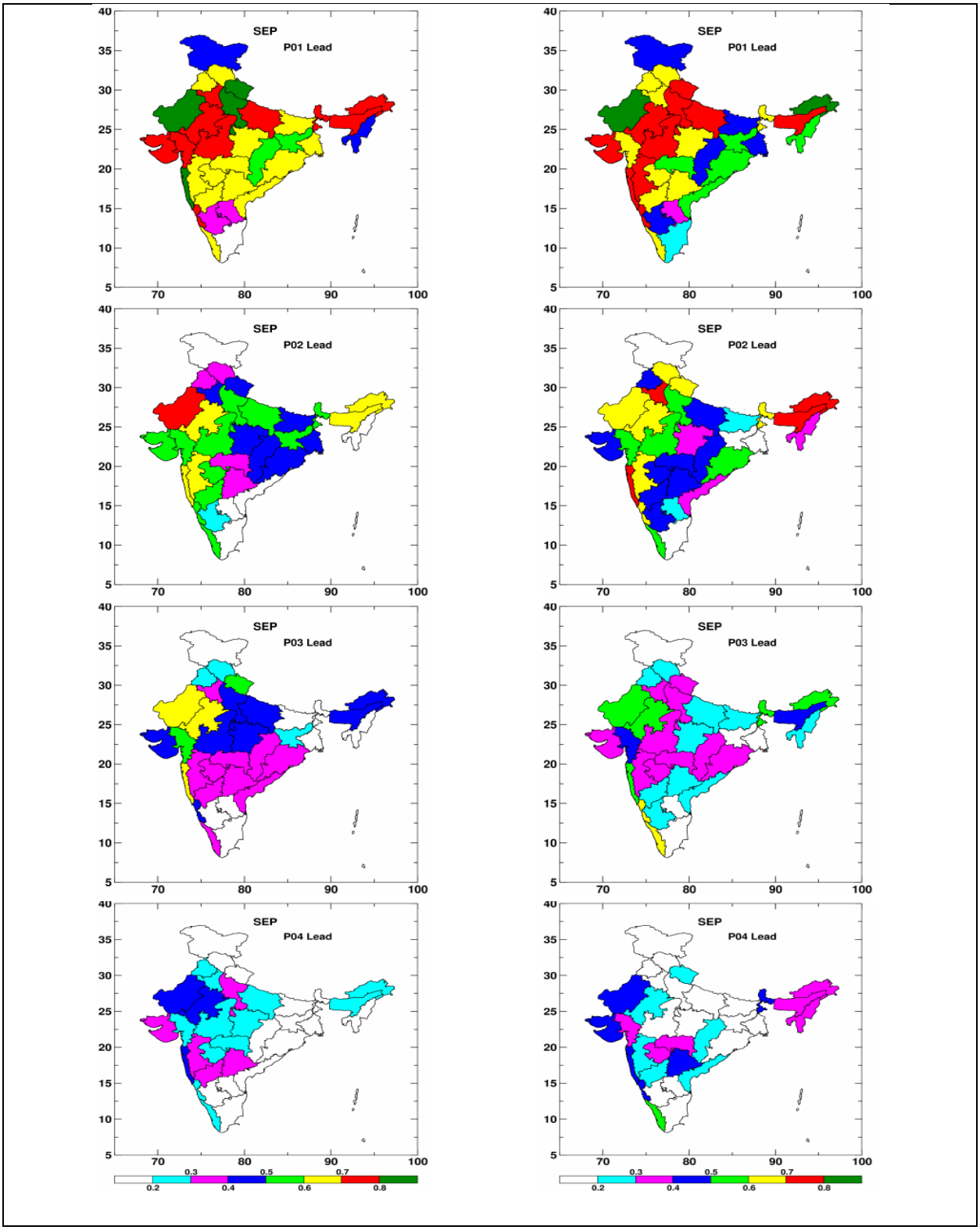

Figure 10: Same as figure 8 but for the month of September.

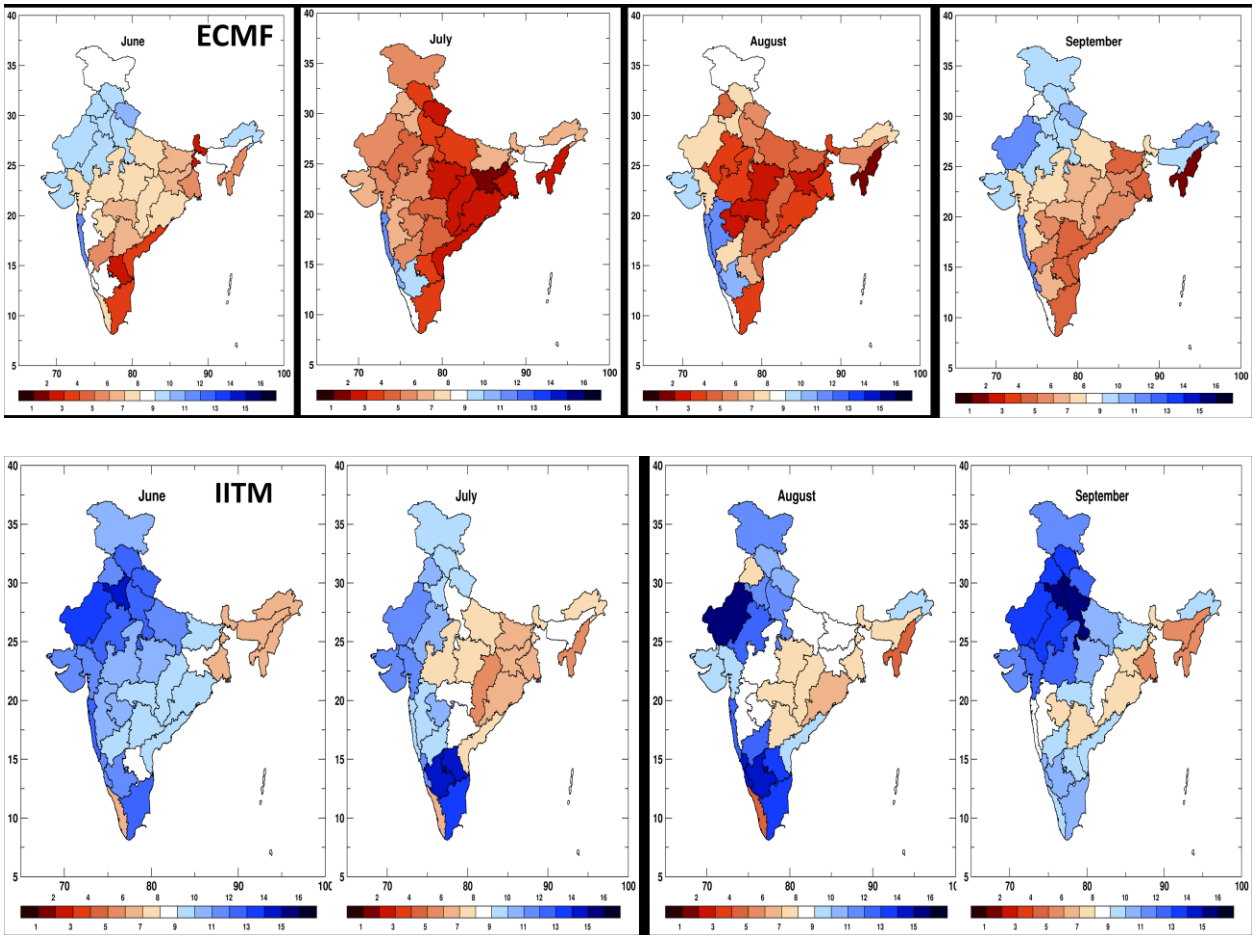

Figure 11: subdivision wise spatial pattern of the days (shaded) in ECMF ENS and IITM MME runs when the signal is equal to noise.

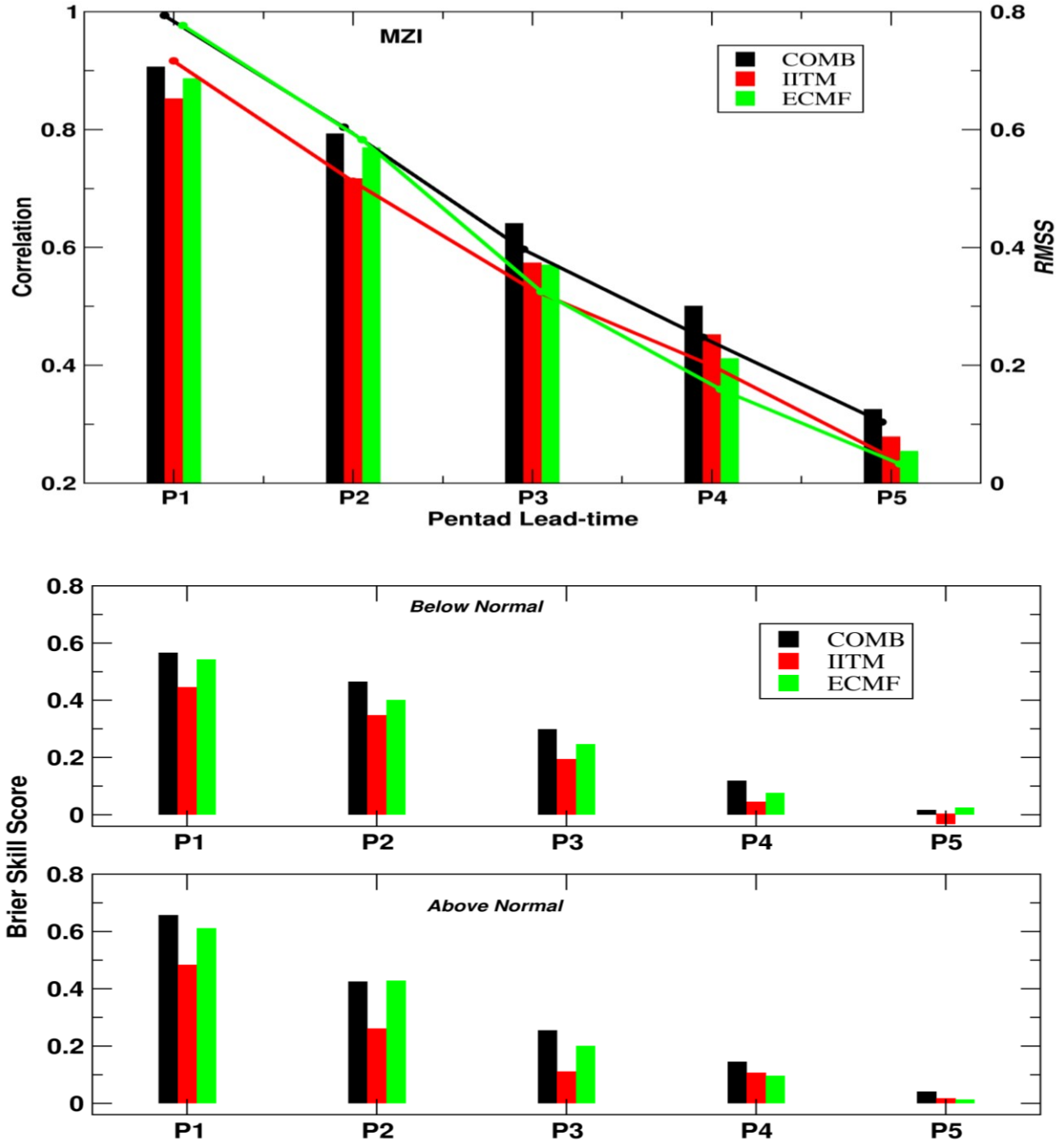

Fig.12. (top) Deterministic skill scores: correlations (bars) and rmss(lines) for the all of the IITM and ECMF combined (COMB), IITM MME and ECMF ENS forecasts and, (bottom) Brier skill score for the core monsoon zone of India (MZI).